Extended Data Fig. 1

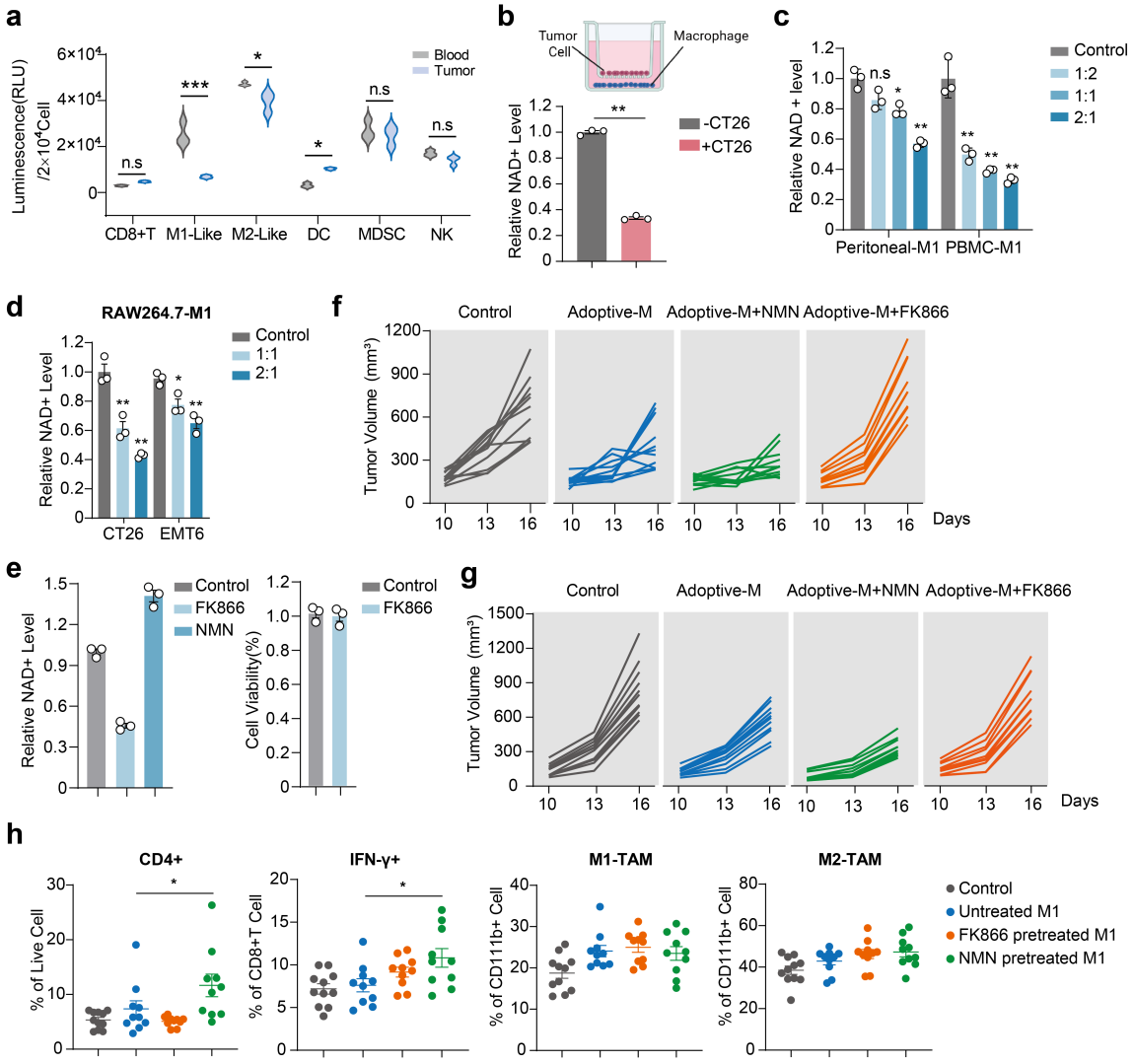

Extended Data Fig. 1. Tumor-induced NAD^+ level alteration in the tumor-infiltrating immune cells. a, Comparison of NAD^+ level in immune cells isolated from peripheral blood versus tumor tissues of EMT6-bearing mice (n = 3). **b,** NAD^+ levels in BMDM-M1 after co-cultured with CT26 cells for 48 h. **c,** NAD^+ levels in M1-like macrophages derived from mouse peritoneal cavity or mouse PBMC cells after exposure to CT26-derived CM at indicated dilutions (v/v) for 48 h. **d,** NAD^+ levels in M1-like macrophages derived from RAW264.7 after exposure to CM of indicated tumor cell lines at indicated dilutions (v/v) for 48 h. **e,** NAD^+ levels or cell viability of BMDM-M1 after treated with NMN (200 μM) or FK866 (50 nM) for 24 h. **f-g**,Tumor growth curve of individual mouse following adoptive transfer of NAD^+-modulated BMDM-M1 in EMT6 (**f**) and 4T1 (**g**) models. Data are mean ± SEM. Statistical significance was assessed using two-way ANOVA followed by Sidak's multiple comparisons

test in **a**, unpaired two-tailed Student's t-test in **b**, and one-way ANOVA followed by Sidak's multiple comparisons test in **c**, **d** and **h.** $^{*}p < 0.05$, $^{**}p < 0.01$, $^{***}p < 0.001$, n.s, not significant.

Extended Data Fig. 2

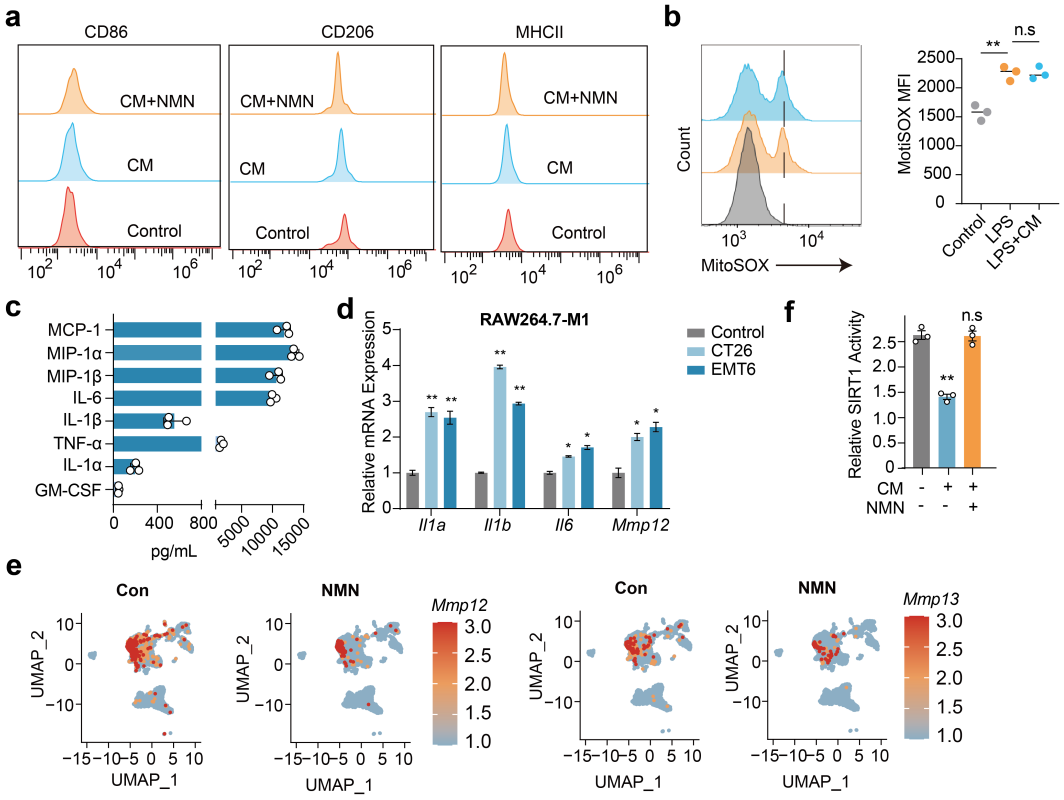

Extended Data Fig. 2. NAD$^+$ decline in M1-macrophages drives SASP. a, Flow cytometry analysis for indicated surface markers of BMDM-M1 after exposure to CT26-conditioned medium (CM) for 24 h. **b,** Representative histograms and quantification of MitoSOX staining in BMDM-M1 after exposure to CT26-CM for 24 h. **c,** ELISA analysis of cytokine concentrations in the supernatants of BMDM-M1 after exposure to CT26-CM for 24 h. **d,** qPCR analysis of SASP gene expression in RAW264.7-M1 after exposure to CT26 or EMT6-derived CM for 24 h. **e,** scRNA-seq analysis of CT26 tumors showing the expression of SASP-related factors. **f,** Intracellular SIRT1 activity in CM-treated BMDM-M1 in the presence or absence of NMN. Data are mean ± SEM. Statistical significance was assessed using one-way ANOVA followed by Sidak's multiple comparisons test in **b**, **d** and **f**. $^{*}p < 0.05$, $^{**}p < 0.01$, $^{***}p < 0.001$, n.s, not significant.

Extended Data Fig. 3

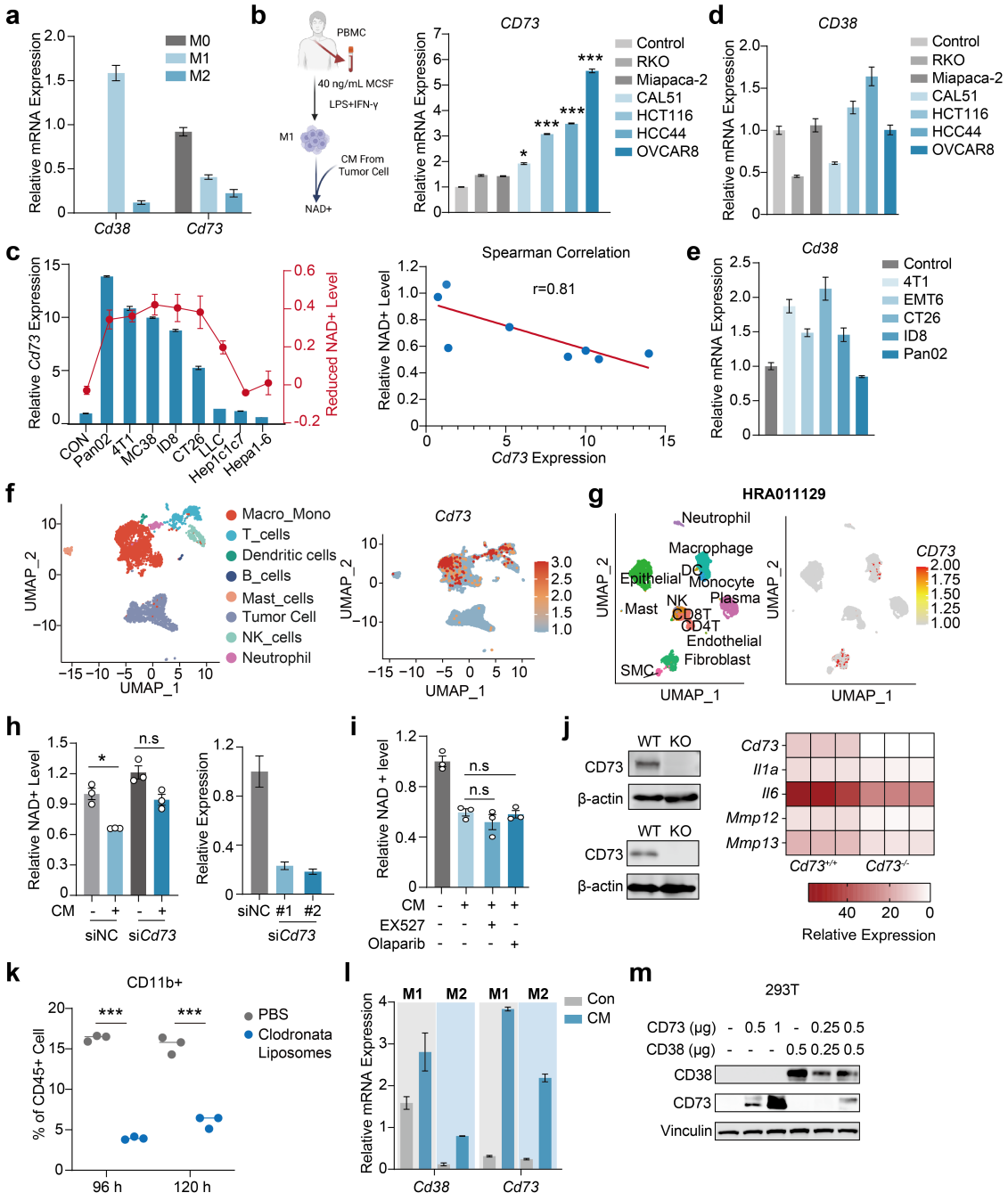

Extended Data Fig. 3. Tumor-induced CD73 accelerates CD38-catalyzed intracellular NAD$^+$ degradation in M1-like macrophages. a, qPCR analysis of CD38 and CD73 expression in BMDM polarized into M0, M1 or M2 states. **b-c,** CD73 expression in human PBMC-M1 (**b**), and CD73 expression and intracellular NAD$^+$ levels in murine BMDM-M1 (**c**) after exposure to conditioned medium (CM) derived from a panel of human or murine tumor cells for 48 h. Correlation analysis between fold changes in CD73 expression and intracellular NAD$^+$ levels.

Spearman correlation coefficients are shown. **d-e,** CD38 expression in PBMC-M1 or BMDM-M1 after exposure to CM derived from a panel of human and murine tumor cells for 24 h. **f,** scRNA-seq analysis reveals the expression landscape of *CD73* across distinct cell populations within CT26 tumors. **g,** Analysis of a human ovarian cancer scRNA-seq dataset (HRA011129) reveals the expression pattern of CD73 across distinct tumor populations. **h,** NAD^+ levels in BMDM-M1 transfected with si*Cd73* (#1, #2) or negative control (siNC) before exposure to CT26-derived CM for 48 h. **i,** NAD^+ levels in BMDM-M1 treated with SIRT1 inhibitor EX523 (10 μM) or PARP inhibitor olaparib (10 μM) before exposure to CT26-derived CM for 48 h. **j,** SASP-related gene expression in $Cd73^{+/+}$ versus $Cd73^{-/-}$ BMDM-M1. $Cd73^{+/+}$ and $Cd73^{-/-}$ BMDM-M1 were treated with CT26-derived CM for 48 h. CD73 protein expression was analyzed by immunoblotting (left), and SASP-related gene expression change were presented as a heatmap (right). **k,** Flow cytometry analysis of splenic $CD11b^+$ myeloid cells after clodronate liposome (200 μL per mouse) treatment in C57BL/6 mice. Shown are representative results of three mice. **l,** *Cd73* expression in M1- or M2-BMDM after exposure to CT26-derived CM for 24 h. **m,** Expression levels of CD38 and CD73 in 293T cells transfected with increasing amounts of plasmid. 0.5 μg of each plasmid encoding CD38 and CD73 was used for measurement of the intracellular NAD^+. Data are mean ± SEM. Statistical significance was assessed using one-way ANOVA followed by Sidak's multiple-comparisons test in **b** and **i**, and two-way ANOVA followed by Sidak's multiple-comparisons test in **h** and **k**. $^*p < 0.05$, $^{**}p < 0.01$, $^{***}p < 0.001$**,** n.s, not significant.

Extended Data Fig. 4

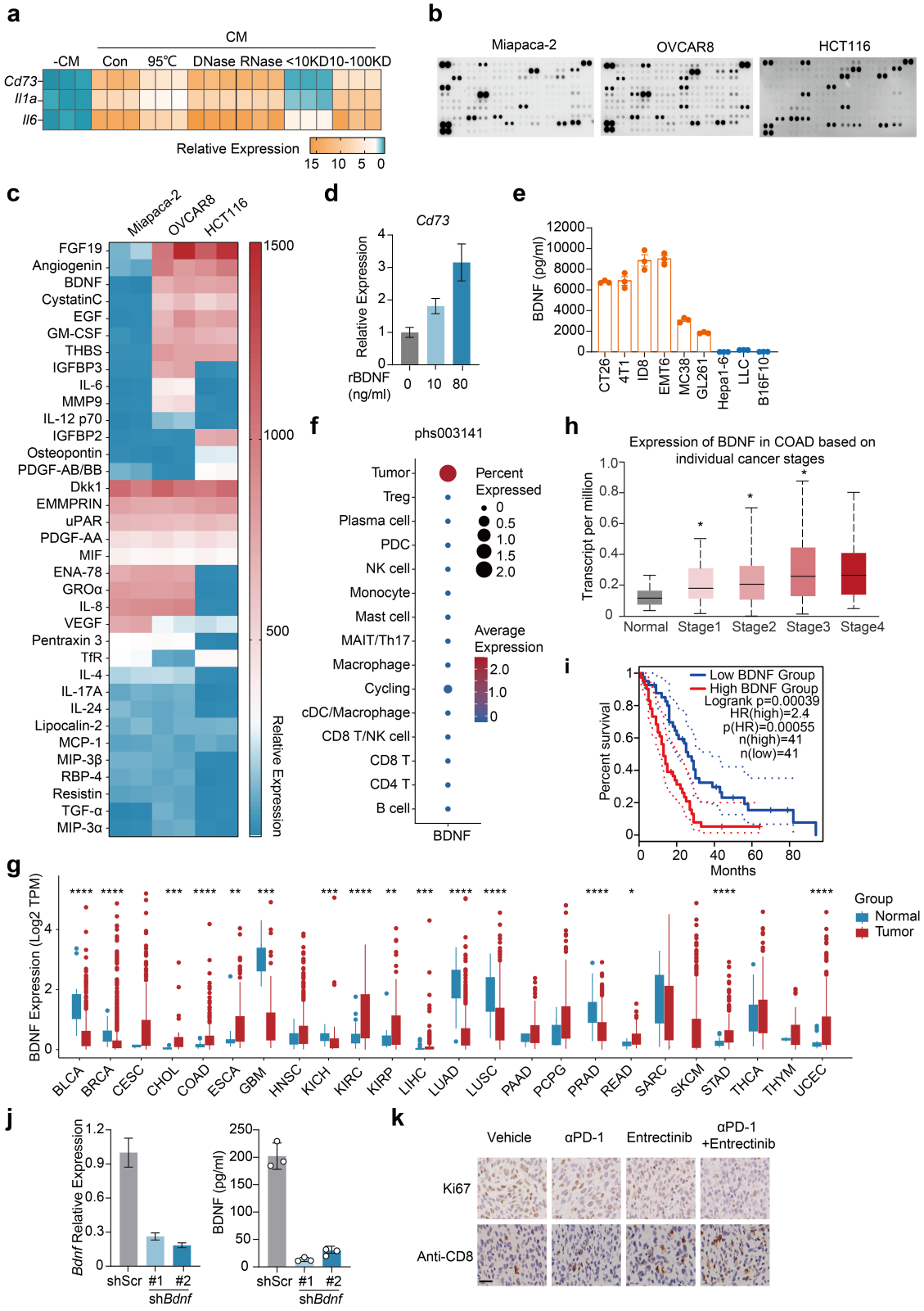

Extended Data Fig. 4. Tumor-secreted BDNF upregulates CD73 in M1-like macrophages.

a, CT26-conditioned medium (CM) was subjected to heat inactivation (95°C, 10 min), DNase (10 μg/mL, 37°C, 1 h), RNase (10 μg/mL, 37°C, 1 h), or size exclusion using a 10-kDa cutoff

filter prior to treatment of BMDM-M1. CD73 and SASP-related gene expression were analyzed after 24 or 48 h, respectively. **b-c,** Differentially secreted proteins in CM from Miapaca-2, HCT116, and OVCAR8 cells. Shown are representative protein array images (**b**) and semi-quantification (**c**). **d,** *Cd73* mRNA expression in murine BMDM-M1 treated with BDNF at gradient concentrations for 24 h. **e,** Quantification of tumor-secreted BDNF in supernatants from a panel of murine tumor cell lines by ELISA. **f,** scRNA-seq analysis of BDNF expression across cell types using published datasets from gastroenteropancreatic neuroendocrine tumors (phs003141). **g,** Analysis of BDNF expression across multiple cancer types using the TIMER database. **h,** Analysis of BDNF expression in colorectal cancer across different tumor stages using the UALCAN database. **i,** Kaplan-Meier survival analysis correlates BDNF expression with prognosis in colorectal adenocarcinoma (COAD) patients using GEPIA database. **j,** BDNF knockdown efficiency in sh*Bdnf* CT26 cells. Shown are qPCR analysis of *Bdnf* mRNA and the concentration of secreted BDNF protein in the supernatant. **k,** Immunohistochemical staining of tumor tissues. Scale bar, 200 μm. Data are mean ± SEM. Statistical significance was assessed using one-way ANOVA followed by Sidak's multiple-comparisons test in **h**. $^{*}p < 0.05$, $^{**}p < 0.01$, $^{***}p < 0.001$. n.s, not significant.

Extended Data Fig. 5

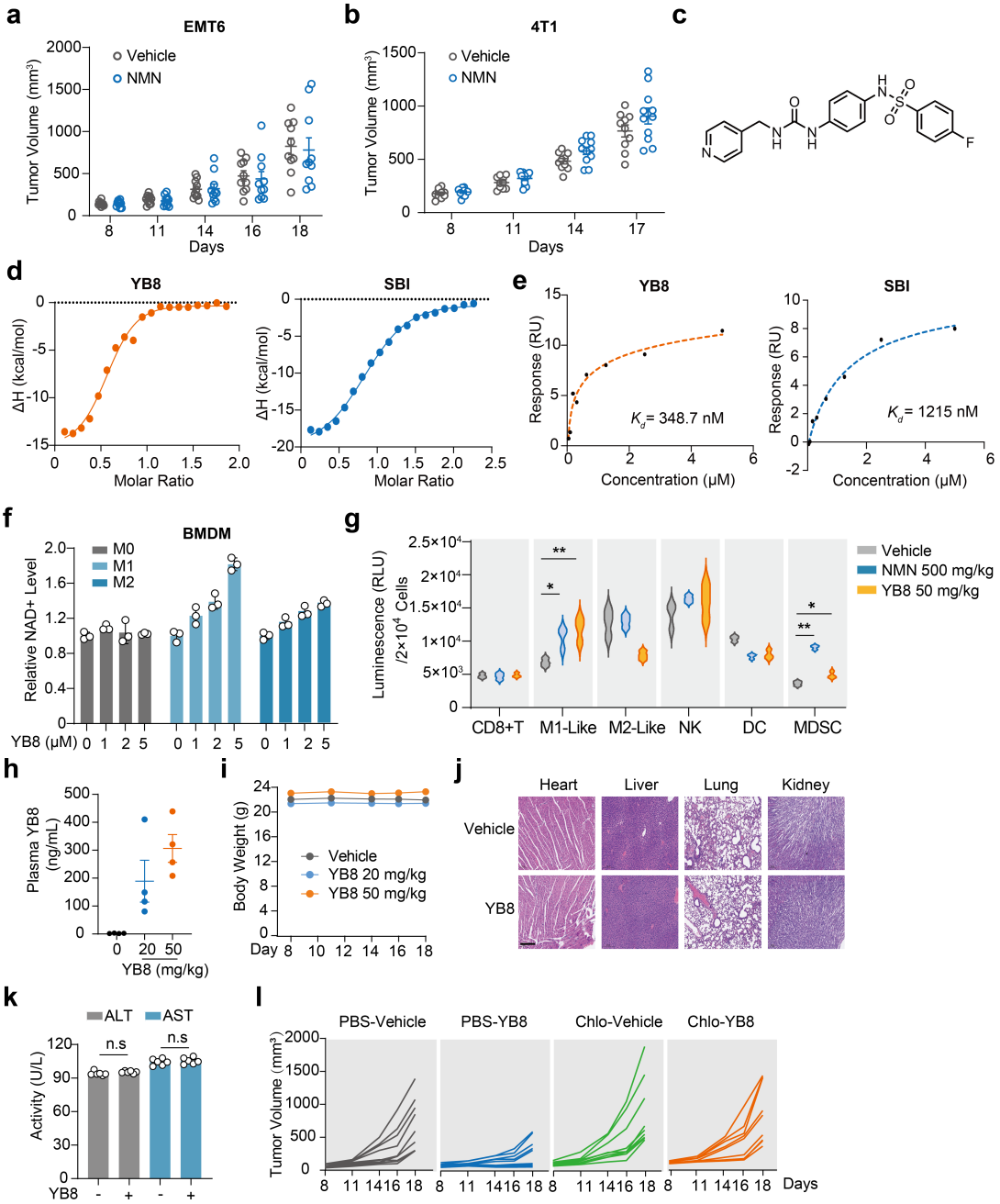

Extended Data Fig. 5. NAMPT activator YB8 rescues tumor-induced NAD$^+$ depletion and restricts tumor growth in a macrophage-dependent manner.

a-b, Tumor growth of EMT6 and 4T1 tumor models upon NMN administration (500 mg/kg, i.p. daily). **c,** Chemical structure of compound YB8. **d-e,** Direct interaction between YB8 and NAMPT protein assessed by isothermal titration calorimetry (ITC) assay and surface plasmon resonance analysis (SPR). SBI was used as a reference compound. **f,** NAD$^+$ fold change in BMDM polarized to M0, M1 or M2 states upon treatment with increasing concentrations of

YB8 for 4 h. **g,** Intracellular NAD^+ levels across different immune cell types isolated from EMT6 tumor-bearing balb/c mice treated with NMN (500 mg/kg, i.p., daily) or YB8 (50 mg/kg, p.o., twice daily) for 10 days (n = 3). **h,** Plasma concentrations of YB8 following oral administration at the indicated doses in EMT6 tumor-bearing mice. **i-k,** Histological and biochemical safety assessment of YB8 treatment regimen. **i**, Mice bodyweight; **j**, H&E staining of major organs (heart, liver, spleen, lung, kidney) collected from mice at the endpoint of the study; Scale bar, 200 μm; **k**, Plasma levels of alanine aminotransferase (ALT) and aspartate aminotransferase (AST). **l,** Tumor growth curves for individual mouse. Data are mean ± SEM. Statistical significance was assessed using two-way ANOVA followed by Sidak's multiple-comparisons test **g** and **k**. $^{*}p < 0.05$, $^{**}p < 0.01$, $^{***}p < 0.001$**,** n.s, not significant.

Extended Data Fig. 6

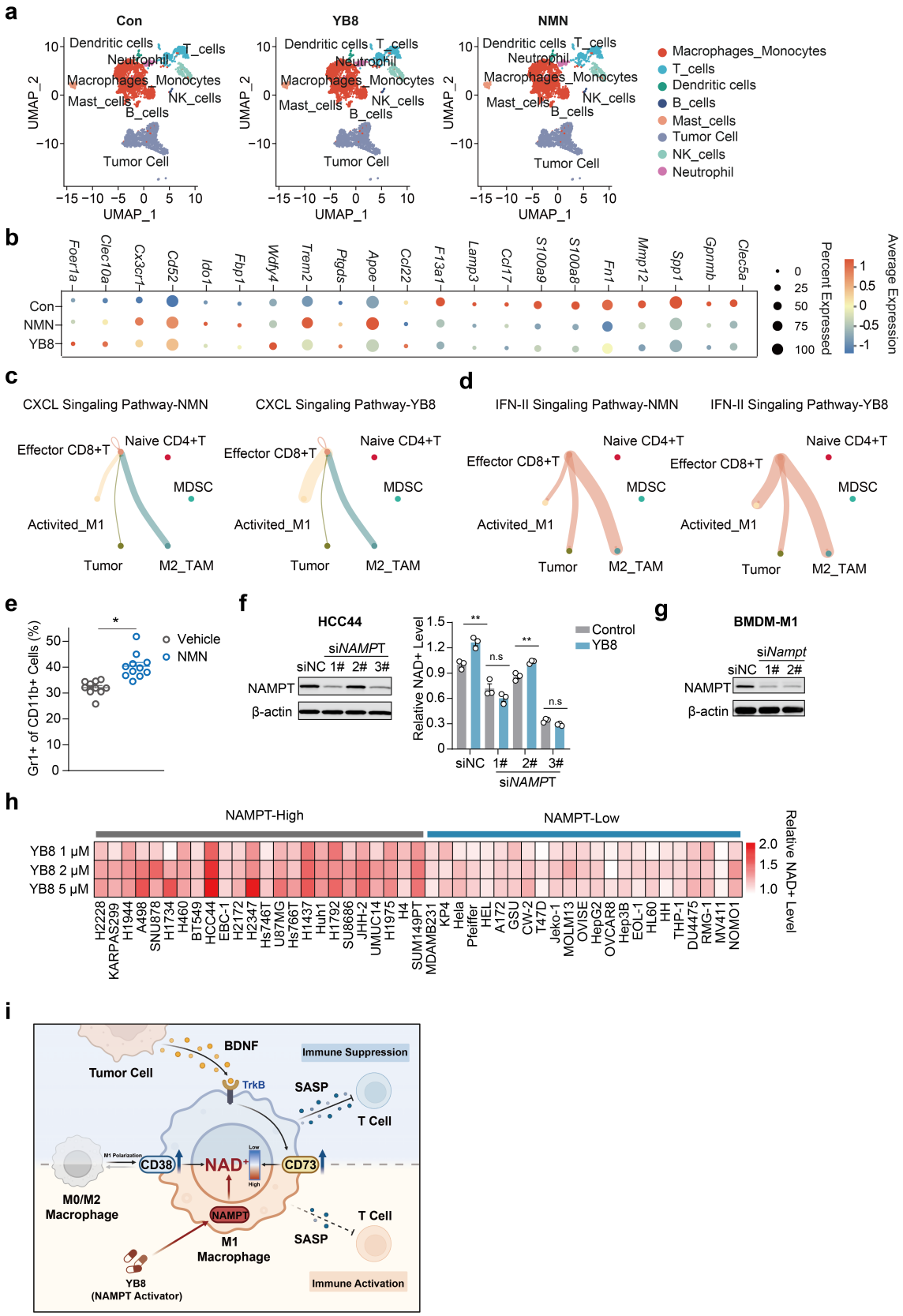

Extended Data Fig. 6. Comparison of tumor immune microenvironment profiles

modulated by YB8 versus NMN. a, scRNA-seq analysis revealed immune cell composition of CT26 tumors upon treatment with YB8 (50 mg/kg, p.o. twice daily) or NMN (500 mg/kg, i.p, once daily) for 15 days. **b,** Expression changes of indicated genes in monocyte/macrophage subpopulations following NMN or YB8 treatment. **c-d,** Comparison of the impact of YB8 and NMN treatment on CXCL and IFN-II mediated signaling directionality and strength across immune cell clusters. **e,** Effects of NMN administration on the proportion of tumor-infiltrating MDSCs in CT26 models. CT26-bearing mice were treated with NMN (500 mg/kg, i.p, once daily) for 15 days. **f,** NAMPT-dependent effect of YB in elevating intracellular NAD^+. HCC44 cells with siRNA knockdown of NAMPT were treated with YB8 treatment (2 μM) for 4 h. **g,** NAMPT known down efficiency in BMDM-M1. **h,** Heatmap depicts intracellular NAD^+ fold changes after 4 h treatment with YB8 (2, 5 μM). **i**, Schematic model of the BDNF-CD73-NAD^+ axis in M1-like macrophages. Tumor-secreted BDNF upregulates CD73 via TrkB signaling. In M1-like macrophages, where CD38 is enriched, CD73 cooperates with CD38 to drive NAD^+ depletion, leading to SASP and impaired $CD8^+$ T-cell function. NAMPT activation (e.g., YB8) restores NAD^+, reversing immunosuppression. Data are mean ± SEM. Statistical significance was assessed using two-tailed unpaired Student's t tests in **e,** or two-way ANOVA followed by Sidak's multiple-comparisons test in **f**. $^*p < 0.05$, $^{**}p < 0.01$, $^{***}p < 0.001$**,** n.s, not significant.